# Heterogeneity and Anisotropy of Injection-Molded Discs of Polypropylene and Polypropylene Composites

S. DÍEZ-GUTIÉRREZ,[1] M. A. RODRÍGUEZ-PÉREZ,[1] J. A. DE SAJA,[1] J. I. VELASCO[2]

[1] Departamento de Física de la Materia Condensada, Cristalografia y Mineralogía, Facultad de Ciencias. Prado de la Magdalena s/n, Universidad de Valladolid, 47011, Valladolid, Spain

[2] Departamento de Ciencias de los Materiales e Ingeniería Metalúrgica, Universidad Politécnica de Cataluña, Barcelona, Spain

*Received 10 August 1998; accepted 10 December 1999*

**ABSTRACT:** The anisotropy and heterogeneity of injection-molded discs of polypropylene, talc-filled polypropylene composites, and silane-treated talc-filled polypropylene composites are studied by means of dynamic mechanical analysis and thermomechanical analysis. The aims of this work are to discover the relationships between the structure of the composites, their anisotropic properties, and the heterogeneity of the molded discs. The experimental results show that although the discs are almost homogeneous, they present a high degree of anisotropy. © 2000 John Wiley & Sons, Inc. J Appl Polym Sci 77: 1275–1283, 2000

**Key words:** polypropylene composites; injection-molded discs; anisotropic properties; talc-filled polypropylene; dynamic mechanical analysis

## INTRODUCTION

Isotactic polypropylene (iPP) has the highest yearly consumption rate among the polyolefins because its property profile can be tailored easily upon request both chemically (polymerization, copolymerization, grafting, reactive blending) and physically (blending, addition of fillers and reinforcements). By a proper upgrading, method the properties of PP meet the requirements of speciality and even those of engineering thermoplastics. The designation of engineering thermoplastics is principally related to a given stiffness (eventual toughness) and heat resistance characteristics (dimensional stability), that can be reached by filling and reinforcing the PP. The resulting PP grade has found widespread applications in the fields of automotive, appliances, and household items.

Talc is the most widely used filler for PP.[1] Its addition began because it made the composites cheaper to produce. Later, however, it was found that it introduced some peculiar properties to the final composites: a higher stiffness and working temperature range, a bigger strength and flexion resistance, a higher thermal conductivity, and a smaller thermal expansion.[2]

In studying the complex structure and morphology of polymers modified by mineral fillers, some problems may arise concerning the characters and extend of interaction at the polymer–filler interface, the heterogeneity of filler distribution, the filler orientation, and the polymer–filler interaction.[3] Because of that, a great number of coupling agents, such as silanes, have been developed to improve this adhesion.[4]

PP talc composites can be processed easily by injection molding, which is a common method to make products from thermoplastics. The proper-

*Correspondence to:* S. Díez-Gutiérrez (sdg@wfisic.eis.uva.es) or M. A. Rodríguez-Pérez.

Journal of Applied Polymer Science, Vol. 77, 1275–1283 (2000)

ties of the molded product depend on the nature of the filler, its concentration, and the molding conditions. The most important characteristics of the filler are its size, shape, its ability to act as nucleating agent for crystallization, and its ability to adhere to the matrix resin. As it is well known, the interior structure of injection-molded plastics is far from being homogeneous or isotropic. This is true for amorphous polymers as well as for semicrystalline polymers. The structure of injection-molded PP talc composites is especially interesting and important. Because of the different mechanical and thermal histories experienced by the material at different points through the cross-section of the part, there is often considerable gradient of both talc and matrix orientation through the thickness. Frequently, it is possible to identify several layers through the section comprising two outer skins and the core. The flow that takes place in the mold has, as might be expected, a considerable influence on the talc orientation and hence on the mechanical properties of the final part. If the filler particle has a large aspect ratio (talc), it tends to orient in the flowing melt during the molding operation. The opportunities to reorient during solidification in the mold after the flow ceases are limited and considerable orientation remains in the molded product.[5] The presence of preferred orientation in the talc particles will of course cause the properties to be anisotropic.

Moreover, the PP reveals an induced crystalline structure when it is molded processed in the presence of mineral fillers such as talc, mica, calcite, etc.[6] However, this effect is more intense in the case of talc. The plates of talc particles lay parallel to the surface of the mold and this induces a preferential orientation in the morphology of the PP phase. Consequently, the PP phase in the composites could also present anisotropic properties. The influence of the mold geometry has been previously shown in the comparison between the results for ASTM bars (ASTM D3641) and those for ISO (ISO 924) plaques.[7] Clearly, the difference between ASTM bar values and those found in many real moldings needs to be borne in mind when designing real parts. Furthermore, samples taken from different parts of the same molds could have different physical properties, which is a consequence of the possible heterogeneity of the injection-molded parts.

From a practical point of view, the anisotropic properties cause molded parts to warp during cooling. The warpage of molded parts impedes part assembly and decreases the quality of the end products. The heterogeneity of the molded parts is a source of zones with worse mechanical properties.

Keeping the previous notions in mind, in this work an experimental investigation on the anisotropy and heterogeneity of injection-molded discs of neat PP, talc-filled PP, and silane-treated talc-filled PP composites by means of dynamic mechanical analysis (DMA) and thermomechanical analysis (TMA) is presented. The work is focused on the relationships between the structure of the composites, their anisotropic properties, and the heterogeneity of the molded discs.

## MATERIALS AND SAMPLES

Commercial isotactic polypropylene, Isplen-051 (Repsol Química S.A., Spain) was used as a matrix. Its molecular characteristics are as follows: $M_w$ = 248297; $M_w/M_n$ = 6.24; isotacticity = 97%; MFI = 5.4 g/10 min (230°C and 2160 g). Talc LU-1445 (Luzenac, Toulouse, France) was used as a filler in our investigation. Its most important physicochemical properties are: laminar particles (97%), average platelet diameter (22 $\mu$m), specific surface (3.8 $m^2\ g^{-1}$) and density (2.7 $g\ cm^{-3}$).

A mixture of gamma-methacryloxypropyltrimethoxy silane and vinytrimethoxy silane (3 : 1 in volume) containing 1% dicumyl peroxide was used for surface treatment of the mineral. For complete surface wetting, the following amounts per kilogram of talc were required: 240 $cm^3$ of methanol, 60 $cm^3$ of water, and 20 $cm^3$ of silane mixture. After the wetting process, the mineral was dried in an oven for 24 h at 60°C.

PP was initially mixed with a nominal talc content of 40 wt %. Two different mixtures were prepared, one with untreated talc, the other with silane-treated talc. Both mixtures were extruded by a twin-screw APV-2030 equipment. By dilution of these materials with the original PP in a single screw extruder, composites were prepared with nominal talc contents of 20 wt %. The composite with untreated talc is denoted as PPN and the composite prepared with silane-treated talc as PPF.

The PP and both composites were injection-molded in discs of 78-mm diameter and 4-mm thickness (ASTM D-647) in a U-40/30 injection machine (Margarit SL., Barcelona, Spain). The temperature profile of injection was 140, 190, 200,

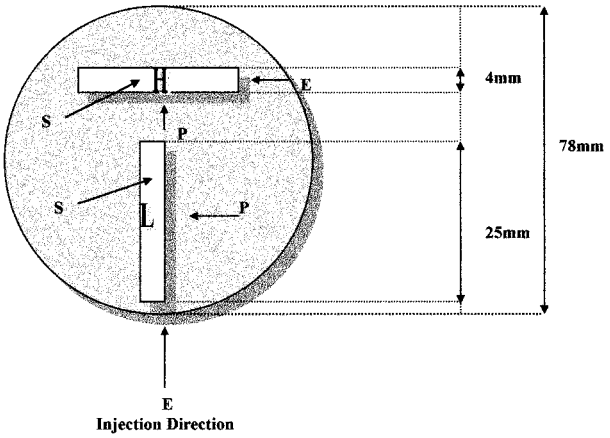


**Figure 1** Nomenclature and dimensions of the samples cut from the injection-molded discs.

and 210°C and the injection pressure was set at 20 MPa.

Two different samples, with dimensions 25 × 4 × 4 $mm^3$, were cut from each injection-molded disc: the sample near the injection point was called "L sample" and the sample far away from this point was called "H sample." The properties of these samples were measured in three perpendicular directions ($S$, $P$, and $E$). The nomenclature used to characterize each sample is shown in Figure 1.

## EXPERIMENTAL

### Scanning Electron Microscopy (SEM)

A Jeol-820 scanning electron microscope was used for morphological observation of freeze-fractured samples after vacuum coating with gold.

### Wide-Angle X-Ray Diffraction (WAXD)

The experiments were performed using a Philips PW 1050/71 diffractometer. Radial scans of intensity ($I$) versus scattering angle ($2\theta$) were recorded in the range 5–70° at a scanning speed, for the detector displacement, of 0.020/0.800 $2\theta$/s by using filtered $CuK_\alpha$ radiation. The scans were taken from the $S$ and $P$ direction of each sample.

### Differential Scanning Calorimetric (DSC)

A Mettler DSC-30 thermal analysis system was used for the thermal characterization. Indium, zinc, and lead standards were used for temperature calibration, whereas the calibration for energy was performed by using indium reference samples. Samples weighing approximately 5 mg were used.

To investigate the influence of the injection processing, the samples were heated up from −50 to 220°C at 10°C/min. On the other hand, to study the activity of the filler and the effect of the coupling agent in the crystallization behavior of the composites, each sample was first heated at 200°C for 4 min to erase any previous thermal history. The calculation of the erasing optimal condition was performed by applying the standard method described by Delvaux and Chambert.[8] The measurements were performed from 200 to 10°C at the following cooling rates: 10, 20, 30, 40, 50, and 80°C $min^{-1}$. From DSC measurements, the crystallinity of the composites and the activity of the fillers were calculated. The crystallinity ($\chi$) was calculated by dividing the measured melting enthalphy ($\Delta H_m$) by the melting enthalpy of 100% crystalline PP ($\Delta H_0 \approx 207.1$ J/g).[9]

$$\chi = \frac{\Delta H_m}{\Delta H_0} \tag{1}$$

To obtain the PP-talc composites' crystallinity, it is necessary to introduce a linear correction factor because of the different content of polymer in each sample. On the other hand, the nonisothermal crystallization experiments were studied following the method developed by Dobreva and Gutzow[10,11] for the study of the crystallization kinetics of molten polymers in the presence of nucleating agents. This method allows obtainment of the parameter $\phi$, that is related to the activity so that a lower value of $\phi$ deals with a higher value of activity.

### DMA

The DMA equipment (Perkin Elmer DMA 7) was calibrated according to the manufacturer's recommended procedures. The storage modulus ($E'$), loss modulus ($E''$), and loss tangent (tan $\delta$) were recorded in a three-point bending measurement system. These properties were measured at 1 Hz, in the temperature range between −40°C and 60°C with a heating rate of 5°C/min. Some previous experiments were performed with lower heating rates (1°C/min and 0.04°C/min) to test the independence of the results with thermal inertia. All the measurements were done in the $S$ and $P$ directions.

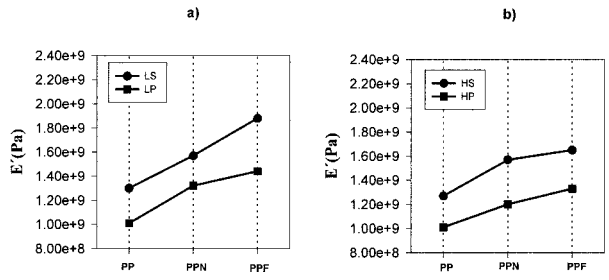


**Figure 2** Average values of the storage modulus at room temperature. (a) *L* samples, (b) *H* samples.

The glass transition temperature ($T_g$) was taken as the temperature of the maximum in the loss tangent curve.[12]

### TMA

In polymeric materials, the thermal transition is accompanied by changes in the coefficient of thermal expansion ($\alpha$). These effects are determined by using TMA, which measures the change in length of a material over a temperature range.

The general thermal behavior of the samples was characterized by temperature scans in all directions (*S*, *P*, and *E*) in the range from −40 to 60°C at 5°C/min. The experiments were conducted on Perkin-Elmer TMA7 test equipment. The applied stress was 130 Pa, sufficient to ensure that the probe remains in contact with the sample and small enough to allow the compression strain to be neglected. The linear thermal expansion coefficient can be determined by:

$$\alpha = \frac{1}{l_1}\frac{l_2 - l_1}{T_2 - T_1} \quad (2)$$

where $l_1$ is the length at a reference temperature $T_1$ ($T_1$ = 25°C in this work) and $l_2$ is the length at $T_2$ ($T_2$ = 30°C).

## RESULTS AND DISCUSSION

### Anisotropy of the Injection-Molded Discs

#### *Dynamic Mechanical Properties*

The values of the storage modulus at room temperature for *L* and *H* samples in the two directions (*S* and *P*) and for all the material under study are shown in Figure 2. The results for both *L* and *H* samples were [$E'$(PPF) > $E'$(PPN) > $E'$(PP)] and [$E'(S) > E'(P)$].

The storage modulus increases always with the addition of the filler, because the talc is a material stiffer than the PP. Besides, the presence of talc produces a more rigid interface in the PP matrix. If the talc is a treated one, the interface will be stiffer. Therefore, the PPF composites have a higher storage modulus than the PPN composites. Figure 2 also shows the behavior of the samples measured in both *S* and *P* directions. The storage modulus is always higher in the *S* direction, even in the case of the PP. The *S*–*P* anisotropy in the PP-talc composites is, in some way, more understandable than in the PP samples. To rationalize these results it is necessary to discuss the structure of the composites.

Figure 3 shows the SEMs of a typical PP-talc sample (PPNLP). These micrographs correspond to a continuous scanning from the surface to the middle of the sample. Injection moldings made from semicrystalline polymers possess skin-core morphology. Although this structure is not distinguished in unfilled PP samples by this technique, the presence of talc makes perfectly visible the skin-core structure in the composites. In Figure 3(a) it is possible to observe a skin zone, where the talc particles lie parallel to the mould surface. After this zone, the talc particles start to follow the flow lines [Fig. 3(b)], until these particles lie perpendicular to the mold surface [Fig. 3(c)]. Considering the entire sample, there are two zones of skin where the talc particles lie parallel to the mold surface and between these two zones a core one, where the talc particles follow the flow lines of the injection process.

On the other hand, this organization can induce a preferential orientation in the morphology of PP crystals placed near the filler, which can be studied by WAXD. To study qualitatively the degree of the *b* axes orientation of the PP unit cell, the ratio of the intensity between the (040) reflection to that of the (110) reflection was obtained.[6,13–17] From the results shown in the Table I, it is deduced that the PP-talc composites measured in the *S* direction, show a strongly favored intensity of the (040) in relation with the (110) reflection. This preferential orientation is much higher in the composites treated with silane.

Furthermore, the plate of the talc particles (001 exfoliation planes) are found parallel to the surface of the mold. This result can be understood taking into account that the ratio between the intensity of the (020) and (002) reflections is higher for the *P* direction. From the previous results, it can be concluded that the talc particles

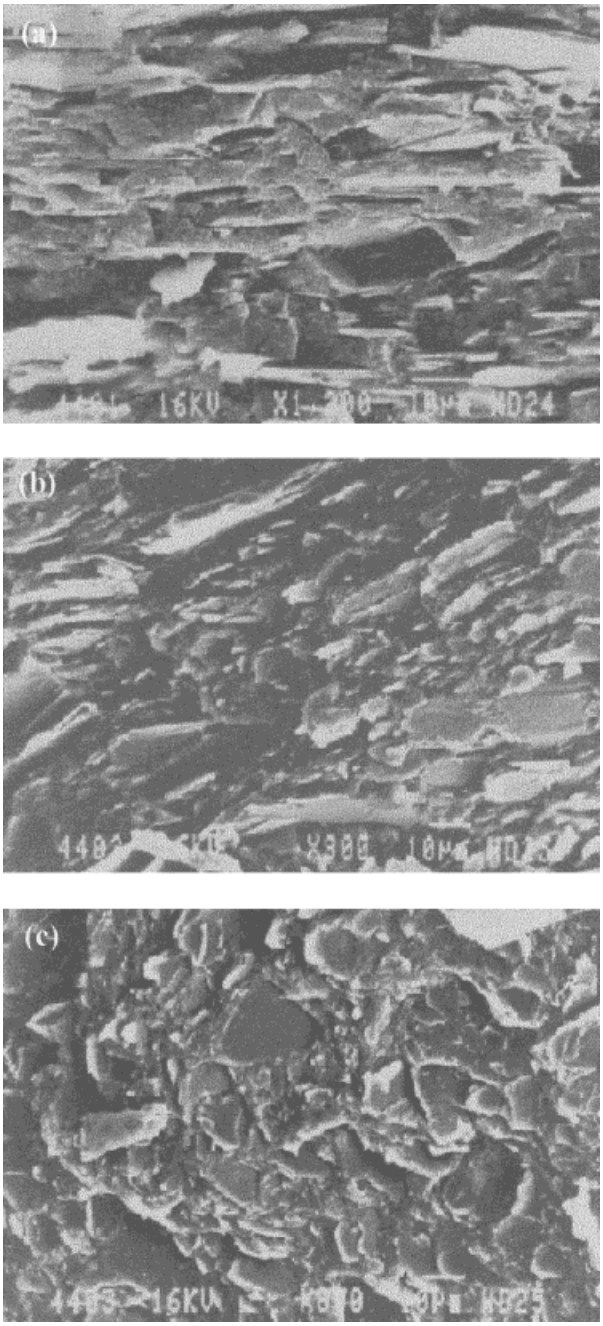


**Figure 3** SEMs of a fractured sample from the surface to the middle of the sample: (a) skin, (b) flow-zone, (c) core.

(001 exfoliation planes) and the $c$ and $a^*$ axes of the PP randomly oriented, are found parallel to the surface of the samples. Consequently, the $b$ axes of the PP unit cell is oriented perpendicular to the surface.

Therefore, when the DMA measurement is performed in the $S$ direction, the particles of talc are perpendicular to the measurement direction and because they are stiffer than the PP, make the deformation process difficult, which results in a higher storage modulus. When the measurement is performed in the $P$ direction, the talc particles are parallel to the measurement direction; as a consequence, they do not offer difficulties to the deformation process and consequently the storage modulus is smaller.

To explain this behavior in the case of the PP samples, it is necessary to take into account that the PP samples under study also showed a nonisotropic crystalline structure. The ratio of the (040) and (110) peaks was approximately 1.19 for the PPLS sample whereas the reported value for the isotropic case was approximately 0.54.[18] Moreover, previous authors[19] have reported that the injection process induces a peculiar skin-core structure in the unfilled PP. In the skin, the $b$ axis of the PP cells is oriented perpendicular to the surface, whereas in the core, the $b$ axis is parallel to the surface. Therefore, when the measurement is performed in the $S$ direction, there is a skin-core-skin structure, which results in two changes of $b$ axis orientation. On the contrary, when the stress is applied in the $P$ direction, there is only a core zone, hence there are not any changes in the $b$ axis orientation. With base on this reasoning, it is logical that the $S$ direction

**Table I Intensity Ratios of (a) Polypropylene (PP), (b) Polypropylene-talc (PPN), and (c) Polypropylene-Talc-Silane (PPF)**

| (a) | PPLS | PPLP | PPHS | PPHP |
|---|---|---|---|---|
| $I(040)$ / $I(110)$ | 1.19 | 0.98 | 1.13 | 0.76 |
| (b) | PPNLS | PPNLP | PPNHS | PPNHP |
| $I(040)$ / $I(110)$ | 5.53 | 0.55 | 5.97 | 0.37 |
| $I(020)$ / $I(002)$ | 0.25 | 5.26 | 0.31 | 3.03 |
| (c) | PPFLS | PPFLP | PPFHS | PPFHP |
| $I(040)$ / $I(110)$ | 20.89 | 0.17 | 18.96 | 0.38 |
| $I(020)$ / $I(002)$ | 0.29 | 5.88 | 0.29 | 4.54 |

The planes (040) and (110) correspond to PP, whereas the planes (020) and (002) are associated with the talc particles.

**Table II Crystallinity (Heating Rate = 10°C/min)**

| Samples | $\chi_c$ (%) |
|---|---|
| PPL | 50.6 |
| PPH | 49.9 |
| PPNL | 49.7 |
| PPNH | 49.9 |
| PPFL | 52.2 |
| PPFH | 53.8 |

presents a higher storage modulus. Besides, the PP-talc composites do not have this change of orientation due to the fact that the *b* axis of PP is oriented perpendicular to the surface in the skin and in the core.[19]

There are two more contributions that it is important to keep in mind to understand the previous results properly. One is the study of the crystalline content of the polymer and how it changes due to the addition of the filler and the coupling agent. The second is the analysis of the amorphous part of the polymer. The first contribution has been studied by means of DSC. Table II summarizes the crystallinity obtained for the different composites. From those results it is clear that $\chi_c(\text{PPF}) > \chi_c(\text{PP}) \geq \chi_c(\text{PPN})$. The crystallinity $\chi$ is almost unaffected by talc filling and considerably increased by the treatment with silanes.[20]

Some conclusions about the amorphous phase of the polymers can be deduced from the $T_g$. The main results were (Table III): $[T_g(S) > T_g(P)]$ and $[T_g(\text{PP}) > T_g(\text{PPN}) > T_g(\text{PPF})]$. The distribution of the talc particles results in lesser mobility of the amorphous phase in the *S* direction; consequently the glass transition takes place at lower temperatures when the measurement is performed in the *P* direction. Despite previous studies about PP + filler composites, where the adding of a filler resulted in a higher $T_g$,[21] our experimental results demonstrate that in the case of PP-talc composites the $T_g$ occurs at lower temperatures. Some experiments were performed at other heating rates to learn whether this result might be a consequence of a thermal delay due to the higher thermal conductivity of the PP-talc composites. Nevertheless, the same tendency was observed.

This might be explained with the aid of the DSC results for the activity of the fillers (Table IV); the talc acts as a nucleating agent, and this

**Table III (a) Values of $T_g$ for All the Samples and All the Directions, (b) Average Values of $T_g$ for PP, PP-Talc, and PP-Talc-Silane**

| (a) Samples | $T_g$ (°C) |
|---|---|
| PPLS | 14.2 |
| PPLP | 10.3 |
| PPHS | 14.3 |
| PPHP | 9.6 |
| PPNLS | 11.0 |
| PPNLP | 7.9 |
| PPNHS | 9.3 |
| PPNHP | 7.9 |
| PPFLS | 7.5 |
| PPFLP | 5.8 |
| PPFHS | 8.1 |
| PPFHP | 8.2 |

| (b) Samples | $T_g$ (°C) |
|---|---|
| PP | 12.1 |
| PPN | 9.0 |
| PPF | 7.4 |

effect is related to a faster crystallization of the PP. This crystallization speed-up causes an amorphous phase with bigger mobility in the PP-talc composites, which results in a lower $T_g$ value. For analogous reasons, the PPF composites (with a higher nucleating effect) have the glass transition at lower temperatures than the PPN composites.

### *Thermal Expansion*

Figure 4 shows the average values of the linear expansion coefficient for all the samples in the three directions: *S*, *P*, and *E*. The main results are: $[\alpha(\text{PP}) < \alpha(\text{PPN}) < \alpha(\text{PPF})$, *S* Direction] and $[\alpha(\text{PP}) > \alpha(\text{PPN}) > \alpha(\text{PPF})$ *P* and *E* Directions]. There is a very small anisotropy *S*-*P*-*E* for the PP. On the contrary, there is a very clear anisotropy *S*-*P*-*E* for the PP-talc composites. The talc crystallizes in flat shape. The *c* axis of the talc is

**Table IV Parameter $\phi$ for the Different Samples**

| Samples | Parameter $\phi$ *L* Samples | Parameter $\phi$ *H* Samples |
|---|---|---|
| PP | 1 | 1 |
| PPN | 0.48 | 0.47 |
| PPF | 0.34 | 0.31 |

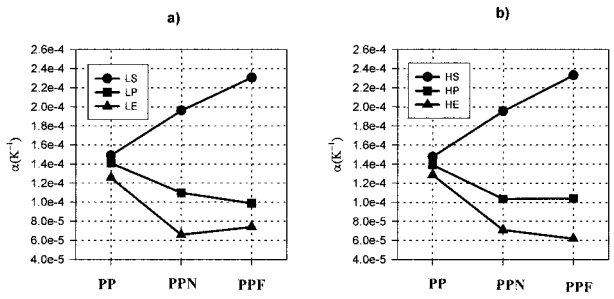


**Figure 4** Linear thermal expansion coefficient for all the samples. (a) *L* samples, (b) *H* samples.

the smallest and it is oriented in the *S* direction. The *a* and *b* axes, the biggest ones, are oriented in the *P* and *E* directions. These results seems to indicate that the talc prevents the polymeric material from expanding in the *P* and *E* directions in which are oriented the bigger dimensions of the talc particles. The restriction in two of the three directions causes the sample to expand in the *S* direction, which explains the increase of the thermal expansion with the addition of talc in this direction. The same result is found when the PP is filled with fibers; the fibers prevent the PP from expanding in the direction of the bigger dimension of the fiber.[22]

## Heterogeneity of the Injection-Molded Discs

### *Thermal Expansion*

According to the definition of *L* and *H* samples (Fig. 1), the heterogeneity of the discs can be analyzed from the different behaviors between samples near the injection point (*L* Samples) and samples far away from this point (*H* Samples).

As can be seen in Figure 5, $\alpha(L) \approx \alpha(H)$ not only for the PP but also for the PP-talc composites. There are nearly no differences between the linear expansion coefficient of both types of samples. Furthermore, as is shown in Figure 4, the expansion is lower in the *E* direction in the *L* and *H* samples. Attending to Figure 1, this result is very peculiar because in the *L* samples, the *E* direction is parallel to the injection direction, whereas in the *H* samples the *E* direction is perpendicular to the injection direction. Taking into account the previous explanations, this result means that the *b* axis of the talc (axis of bigger dimension) is oriented in a different way in *L* and *H* samples. Due to the fact that the biggest restriction is in the *E* direction, the *b* axis of the talc seems to be oriented in the mentioned direction (Fig. 6).

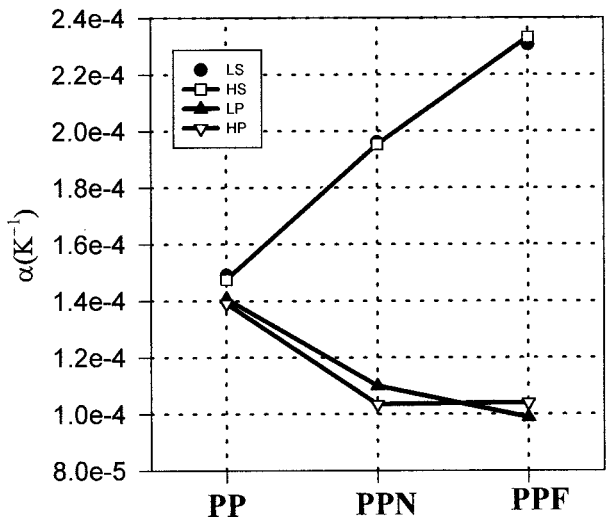


**Figure 5** Linear thermal expansion coefficient. *L*-*H* differences.

### *Dynamic Mechanical Properties*

The storage modulus of the samples as a function of the temperature measured in the *S* and *P* directions is shown in Figure 7. The main results that can be obtained from Figure 7 are: [$E'$(PPL) $\approx$ E′(PPH)] and [$E'$(PPNL, PPFL) $>$ $E'$(PPNH, PPFH)]. The storage modulus of the *L* samples is higher than that of the *H* samples for the PP-talc composites. This result can be explained with the results obtained by means of SEM (Fig. 8). Figure 8(a,b) shows the micrographs of PPFL and PPFH samples taken at the same distance from the sample surface. The *L* samples seem to have a bigger zone where the talc particles are oriented parallel to the surface, so the skin is thicker in the *L* samples than in the *H* samples. This result has

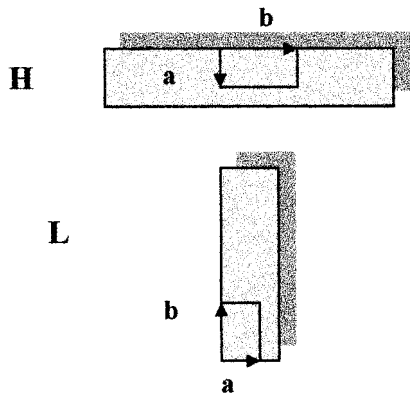


**Figure 6** Orientation of the talc particles in *L* and *H* samples.

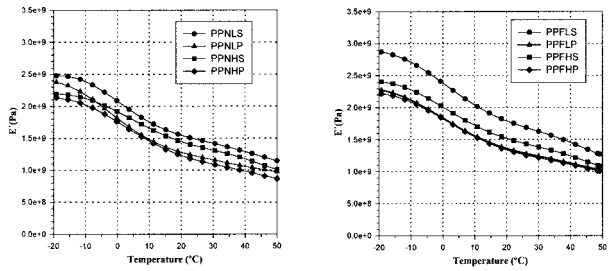


**Figure 7** Storage modulus as a function of the temperature. Differences of *L*-*H* for PP-talc composites.

been verified by means of WAXD measurements. The analysis of the intensity ratio between the (020) and the (002) reflections (planes of talc) in the *P* direction, show that this ratio is bigger for the *L* samples. This means that the plane (020) is more parallel to the surface of the mold in the *L* samples. Furthermore, from Figure 7 it is also clear that the *L*-*H* differences are greater in the *S* than in the *P* direction. When the measurement is performed in the *S* direction, the sample presents a skin zone + core zone + skin zone, whereas the *P* direction only presents a core zone. Therefore, it seems to be reasonable that the heterogeneity of the injection discs was bigger in the *S* direction.

Analyzing the results obtained (Table III), the $T_g$ values are almost the same for *L* and *H* samples $T_g(L) \approx T_g(H)$. There is no differences between this parameter for samples near and far from the injection point. Consequently, it is possible to conclude that *L* and *H* samples do not have important differences between their amorphous phases.

## CONCLUSIONS

An investigation on the heterogeneity and the anisotropy of injection-molded discs of PP, PP-talc and PP-talc functionalized with silanes has been presented. DMA and TMA have been used to characterize the macroscopic behavior of the samples in the different directions (*S*, *P*, *E*) and from different zones of the disc (*L*, *H*). To help in the interpretation of the measured macroscopic parameters, some microscopic experiments have been performed by means of DSC, SEM, and WAXD.

The experimental results have shown that although the discs are almost homogeneous they present a high degree of anisotropy.

The injection molded disc of PP-talc composites present a small heterogeneity that can only be appreciated in the storage modulus. The *L* samples have a higher storage modulus than the *H* samples, which can be explained by a greater orientation of the talc particles (thicker skin zone).

The anisotropy of the injection-molded discs is very high. For all the samples (PP, PPN, PPF) the storage modulus is higher when the measurement is performed in the *S* direction.

The values of the linear expansion coefficient for the PP are very similar in the three directions: *S*, *P*, *E*. Instead of this, for the PP-talc composites, this parameter presents a very clear anisotropy. The filler prevents the PP matrix from expanding in a different way depending on the dimension of the talc particles. The *E* and *P* directions present smaller linear expansion coefficient for the PP-talc composites than for the PP, whereas in the *S* direction, the opposite takes place.

The differences between the injection disc of PP and PP-talc composites are very clear. The

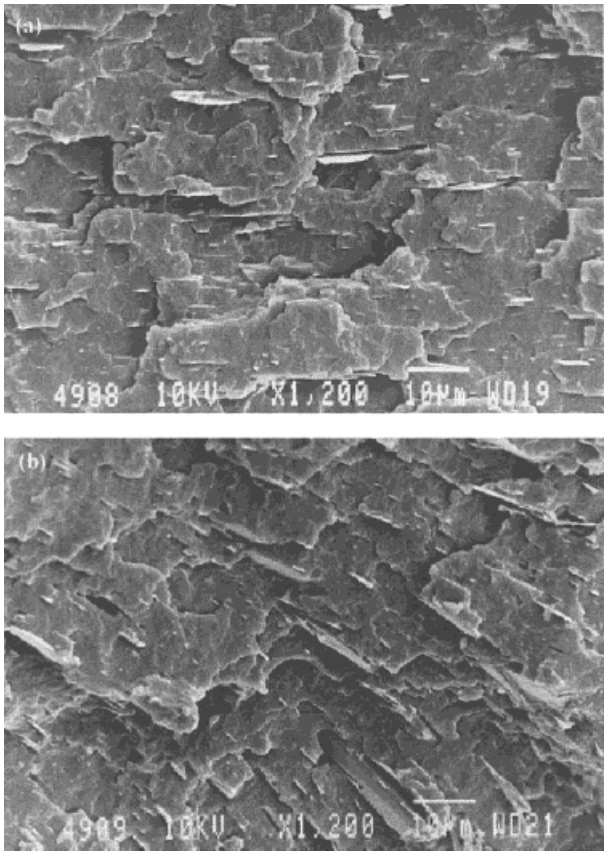


**Figure 8** SEMs of fractured samples in the skin zone: (a) PPFL, (b) PPFH.

storage modulus increases always with the addition of talc because of the bigger stiffness of the talc and because the talc generates a stiffer interface in the PP matrix. With the treated talc, this interface is stiffer, which results in a higher storage modulus for the treated discs. The nucleating effect of the talc is related to a faster crystallization of the polymer, which results in an amorphous phase with a bigger mobility (lower $T_g$).

## REFERENCES


1. Vink, D. Kunststoffe 1990, 80, 842–846.
2. Fujiyama, M.; Wakino, T. J Appl Polym Sci 1991, 42, 2739–2747.
3. Fujiyama, M.; Wakino, T. J Appl Polym Sci 1991, 42, 9–20.
4. Velasco, J. I.; Saja, J. A.; Martínez, A. B. J Appl Polym Sci 1996, 61, 125–132.
5. Morales, E.; White, J. R. J Mat Sci 1998, 23, 4525–4533.
6. Fujiyama, M.; Wakino, T.; Kawasaki, Y. J Appl Polym Sci 1988, 35, 29–49.
7. Gibson, A. G. In Polypropylene Structure, Blends and Composites; J Karger-Kocsis, Ed.; Chapman & Hall: London, 1995; Vol. 3.
8. Delvaux, E.; Chambert, B. Polym Commun 1990, 31, 391–394.
9. Wunderlich, B. Thermal Analysis; Academic Press: New York, 1990; p 418.
10. Dobreva, A.; Gutzow, I. J Non-Cryst Solids 1993, 162, 1–12.
11. Dobreva, A.; Gutzow, I. J Non-Cryst Solids 1993, 162, 13–25.
12. Rotter, G.; Ishida, H. Macromolecules 1992, 25, 2170–2176.
13. Chen, Z.; Finet, C.; Liddell, K.; Thompson, D. P.; White, J. R. J Appl Polym Sci 1992, 46, 1429–1437.
14. Menzik, Z.; Fitchmun, D. R. J Polym Sci Polym Phys Ed 1973, 11, 973.
15. Fujiyama, M.; Wakino, T. J Appl Polym Sci 1991, 42, 2739–2747.
16. Fujiyama, M.; Wakino, T. J Appl Polym Sci 1991, 43, 57.
17. Fujiyama, M.; Wakino, T. J Appl Polym Sci 1991, 43, 97.
18. Addink, E. J.; Beintema, J. Polymer 1961, 2, 185–193.
19. Fujiyama, M. In Polypropylene: Structure and Composites; Karger-Kocsis, J., Ed. Chapman & Hall: London, 1995; Vol. 1.
20. Velasco, J. I.; Saja, J. A.; Martinez, A. B. J Appl Polym Sci 1996, 61, 125–132.
21. Hartmann, B. In Sound and Vibration Damping with Polymers; Corsaro, R. D., Sperling, L. H., Eds.; American Chemical Society: Washington, DC, 1990.
22. Hindle, C. S.; White, J. R.; Dawson, D.; Thomas, K. Polym Eng Sci 1992, 32, 155–171.